Research Article

PM$_{2.5}$-bound Inorganic and Nonpolar Organic Compounds in Chuncheon, Korea

Sung-Won Park[1], Young-Ji Han[1],*, Jin-Hyuk Hong[2], Tae-Hyung Lee[3]

[1]Department of Environmental Science, Kangwon National University, Chuncheon 24341, Republic of Korea
[2]Department of Integrated Particulate Matter Management, Kangwon National University, Chuncheon 24341, Republic of Korea
[3]Department of Environment, Hankuk University of Foreign Studies, Yongin 17035, Republic of Korea

*Corresponding author.
Tel: +82-33-250-8578
E-mail: youngji@kangwon.ac.kr

Received: 16 November 2022
Accepted: 5 December 2022

ABSTRACT　In this study, major chemical components of PM$_{2.5}$ including nitrate, sulfate, organic carbon (OC), and elemental carbon (EC) were measured in Chuncheon, South Korea in May–June, 2021. Average PM$_{2.5}$ concentration was 16.4 ± 9.7 µg m^{-3}, and OC was the largest contributor of PM$_{2.5}$ mass concentration. High concentration episodes (HCEs), defined when PM$_{2.5}$ concentration exceeded 30 µg m^{-3}, were caused by Asian dust, secondary inorganic aerosol (SIA) formation, and primary OC emission. NH$_4^+$ was determined to be a limiting factor for SIA formation based on neutralization ratio. There was statistically significant correlation between n-alkanes and PM$_{2.5}$, and odd alkanes including C27, C29, and C31, which are generally emitted from biogenic sources, were abundant species, suggesting the importance of natural sources over fossil fuel combustion. Polycyclic aromatic hydrocarbons (PAHs) concentrations were significantly lower than those measured at the same sampling site in 2014–2015. Based on the diagnostic ratios of PAHs, vehicular emission, rather than solid fuel emission, were significant for PAHs. Detailed characterization of chemical composition of PM$_{2.5}$ reported in this study can be of great help in establishing an appropriate abatement policy to reduce PM$_{2.5}$ concentrations.

KEY WORDS　PM$_{2.5}$, Organic carbon, N-alkanes, Polycyclic aromatic hydrocarbon, Secondary inorganic aerosol

1. INTRODUCTION

Particulate matter with aerodynamic diameter less than or equal to 2.5 µm (PM$_{2.5}$) adversely affects human health, causing various pulmonary and cardiovascular diseases (Pun *et al.*, 2017; Atkinson *et al.*, 2014; Hoek *et al.*, 2013; Dominici *et al.*, 2006). In fact, PM$_{2.5}$ has been one of the most significant air pollutants in East Asia for more than a decade. Its concentration in South Korea showed a decreasing trend until 2012, and since then has become stagnant. The current annual national ambient air quality standard of Korea is 15 µg m^{-3}, and the PM$_{2.5}$ concentrations measured at most national air quality monitoring stations, regardless of urban area, industrial city, or small residential city, exceed its national standard (NIER, 2022a), and are more than 4 times higher than the WHO guideline (WHO, 2021). Many studies have suggested that a large portion of PM$_{2.5}$ in South Korea is affected by

the long-range transport from China (Choi *et al.*, 2022; Byun *et al.*, 2020; Lee *et al.*, 2019); however, $PM_{2.5}$ concentrations in Korea have been stagnant since 2013, whereas due to the stringent mitigation efforts, they were dramatically reduced in eastern China from 2013 to 2019 (Li *et al.*, 2020; Zeng *et al.*, 2019).

The various components that $PM_{2.5}$ is composed of include ionic compounds, organic matter, elemental carbon, and metallic components, which are either emitted from natural and anthropogenic sources, or formed secondarily via atmospheric reactions. Ionic compounds, including $(NH_4)_2SO_4$, NH_4HSO_4, and NH_4NO_3, are predominantly formed in atmosphere by gaseous precursors, such as NH_3, NOx, and SO_2. Organic aerosol (OA), a major component of $PM_{2.5}$, consists of more than 1,000 individual organic components; OA can be divided into primary organic aerosol (POA) directly emitted from various sources, and secondary organic aerosols (SOA) generated through various homogeneous and heterogeneous reactions with oxidants (Xing *et al.*, 2019; Seinfeld and Pandis, 2016; Tsimpidi *et al.*, 2010). Organic tracers are generally divided into polar and nonpolar organic compounds, and nonpolar organic compounds such as alkanes and polycyclic hydrocarbons (PAHs) have been studied for identifying primary emission sources. N-alkanes are relatively stable and emitted from both anthropogenic and biogenic sources (Zhang *et al.*, 2021; Kotianová *et al.*, 2008). PAHs are mainly emitted from incomplete combustion of liquid fuel such as gasoline and diesel and solid fuels such as biomass and coal (Yan

et al., 2019).

This study was performed in a small-sized inland residential city, Chuncheon, South Korea. According to the national emissions inventory, the emission rates of the major air pollutants including $PM_{2.5}$ in this city are very low compared with adjacent cities; however, $PM_{2.5}$ consistently showed similar or even higher concentrations than in Seoul and other large cities (NIER, 2022b). To identify the cause of high $PM_{2.5}$ concentrations, daily $PM_{2.5}$ and its chemical constituents were measured from May 14 to June 26, 2021. Detailed characterization of chemical composition can be of great help in identifying the possible sources and/or formation pathways of $PM_{2.5}$, and in establishing an appropriate abatement policy.

2. METHODOLOGY

2.1 Site Description and Sampling

Samples of $PM_{2.5}$ were collected on the roof of a four-story building of Kangwon National University (KNU) in Chuncheon, South Korea (37°87′N; 127°74′E) (Fig. 1). Chuncheon is a medium-sized residential city without large-scale anthropogenic sources, and is therefore expected to be affected more by regional- or long-range transport from the metropolitan and industrial areas located in the northwestern part of South Korea (Fig. 1). Samples of $PM_{2.5}$ were collected for 23 h from 10 am to 9 am the following day from May 15, 2021 to June 26, 2021. To quantify $PM_{2.5}$ mass concentration, a 47 mm
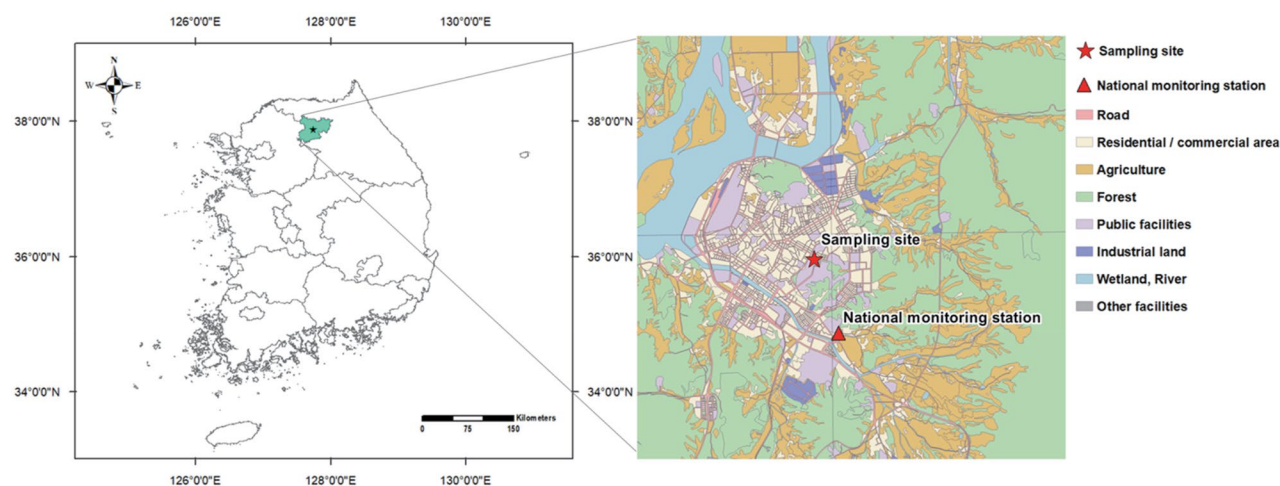

Fig. 1. The sampling location of this study in South Korea (left) and an enlarged map around the sampling site in Chuncheon (right). The nearest national air quality monitoring station was also indicated.

PTFE membrane filter with supported polypropylene ring (pore size of 2.0 μm, GVS, Italy) and a cyclone were used in a PMS-204 sampler (APM Engineering, Bucheon-si, Korea) at a flow rate of 16.7 L min^{-1}. Carbonaceous components were collected on a pre-baked 47 mm quartz filter (pore size of 2.2 μm, Whatman, Maidstone, UK) with a carbon denuder (Sunset Laboratory Inc., USA) and a cyclone at a flow rate of 16.7 L min^{-1}. High volume air sampler (Hi-vol 3000, Ecotech, Australia) with quartz filter (203.2 mm × 254 mm) was used to measure organic compounds. For ionic compounds, a 47 mm PTFE filter (pore size of 1.0 μm, GVS, Italy) was used with a cyclone and two 3-channel annular denuders (URG-2000-30x242-3CSS, URG Co., Chapel Hill, NC, USA) at a flow rate of 10 L min^{-1}. The annular denuder was coated with citric acid solution (100 mL of ethanol + 1 g of citric acid + 1 g of glycerol) to remove acid gases (SO$_2$, HNO$_3$, HNO$_2$) and Na$_2$CO$_3$ solution (50 mL of ethanol + 50 mL of ultrapure water + 1 g of Na$_2$CO$_3$ + 1 g of glycerol) to remove NH$_3$.

2.2 Chemical Analysis

The Teflon filter was stored under controlled conditions of temperature (20°C) and RH (50%) for 24 h before and after sampling, and was then weighed three times using a microbalance (readability = 10^{-5} g, CP 225D, Satorius, Germany) equipped with a static eliminator (The Staticmaster 2U500, NRD, USA) to determine PM$_{2.5}$ mass concentration. To analyze ionic compounds, the filters were extracted with 10 mL of ultrapure water in an ultrasonic extractor for 2 h. The extract was filtered with 0.45 μm PTFE syringe filter, and analyzed with ion chromatography (Metrohm AG, Switzerland). For organic carbon (OC) and elemental carbon (EC) analysis, 1.5 m^2 of quartz filter was analyzed using the National Institute of Occupational Safety and Health (NIOSH) method 5040 for thermal-optical analysis. The detailed method can be found in other studies (Byun *et al.*, 2020; Park *et al.*, 2018).

For nonpolar organic compounds, the collected filters from high-volume air sampler were cut into pieces, and

Table 1. Internal standards used and the QA/QC results for PAHs and n-alkanes in this study.

	Compounds	r^2	Recovery (%)	MDL (ng m^{-3})
PAHs	Penanthrene (Phe)	0.999	114	0.002
	Anthracene (Ant)	0.998	63	0.003
	Fluoranthene (Flt)	0.999	99	0.003
	Pyrene (Pyr)	0.999	101	0.002
	Benz[a]anthracene (BaA)	1.000	94	0.011
	Chrysene (Chr)	0.998	96	0.009
	Benzo[b]fluoranthene (BbF)	0.999	93	0.006
	Benzo[k]fluoranthene (BkF)	0.999	94	0.007
	Benzo[a]pyrene (BaP)	0.999	91	0.008
	Indenol[1,2,3-cd]pyrene (IcdP)	0.998	94	0.003
	Benzo[g,h,i]perylene (BghiP)	0.997	95	0.010
n-alkanes	C20 (Eicosane)	0.997	108	0.002
	C21 (Heneicosane)	0.999	77	0.002
	C22 (Docosane)	0.999	94	0.008
	C23 (Tricosane)	0.999	99	0.006
	C24 (Tetracosane)	0.998	103	0.004
	C25 (Pentacosane)	0.998	103	0.007
	C26 (Hexacosane)	0.998	105	0.007
	C27 (Heptacosane)	0.998	94	0.006
	C28 (Octacosane)	0.998	92	0.009
	C29 (Nonacosane)	1.000	81	0.008
	C30 (Triacontane)	1.000	67	0.013
	C31 (Hentriacontane)	0.999	99	0.010
	C32 (Dotriacontane)	1.000	84	0.015
	C33 (Tritriacontane)	0.999	70	0.013
	C34 (Tetratriacontane)	0.999	62	0.010

placed in amber glass vials containing 50 mL of dichloromethane (DCM, GC grade, Fisher chemical, USA)/methanol (HPLC grade, Fisher chemical, USA) mixture (3:1). After injecting internal standards into the vials, the samples were extracted twice in an ultrasonicator for 30 min. The extracts were concentrated to 10 mL at 40°C using N_2 (99.999% purity) gas evaporator (Turbo storm, SCINCO, Korea), filtered by 0.45 μm PTFE syringe filter (Pall Corp., USA), and reduced to the final volume of 0.5 mL at room temperature using a N_2 (99.999%) concentrator. The GC-MS (GC 7890A/MSD 59975C, Agilent Technologies, USA) was used for n-alkanes (C20–C34) and 11 PAHs (Table 1). Table S1 of the Supplementary Information (SI) describes the analysis condition of GC-MS.

2.3 Quality Assurance and Quality Control (QA/QC)

Calibration curve was obtained using 7 different concentrations of standard solutions, and r^2 was higher than 0.997 (Table 1) when using the internal standard technique (NIER, 2011). Acenaphthene-d10 and Pyrene-d10 were used as internal standards for PAHs, while Pentadecane-d32, Eicosane-d42, Tetracosane-d50, Dotriacontane-d66, and Hexatricontane-d74 were used as internal standards for n-alkanes. Method detection limit (MDL) was calculated as 3.14 times the standard deviation by analyzing the standard solution 7 times. The extraction recoveries for n-alkanes and PAHs were determined by spiking the standard solution in the blank filter, and ranged (62 to 114)% (Table 1).

2.4 Meteorological Data and Other Pollutants

Meteorological data (temperature, wind speed, and relative humidity) were measured every 5 min using meteorological equipment (Wireless Vantage Pro2 Weather Station, Davis Instrument, Hayward, CA, USA) at the sampling site. Meteorological data were measured every 5 min, but averaged to match the temporal resolution of $PM_{2.5}$ samples. It should be noted that there are possible uncertainties caused by using different timescales for the measurements of pollutants and for meteorological data. Concentrations of PM_{10} and gaseous pollutants, including O_3, NO_2, SO_2, and CO, were observed from the nearest national ambient air quality monitoring station, which is located about 1.5 km distance from the sampling site (Fig. 1).

3. RESULTS AND DISCUSSION

3.1 Characterization of High-concentration Episodes

Average $PM_{2.5}$ concentration was (16.4 ± 9.7) μg m^{-3}, and OC showed the highest concentration (3.2 μg m^{-3}), contributing about 20% of total $PM_{2.5}$ mass. The SO_4^{2-} was higher than NO_3^-, probably because of active photochemical sulfur oxidation in the warm season (Zhou *et al.*, 2016; Gao *et al.*, 2011). The $PM_{2.5}$ was better correlated with carbonaceous compounds ($r^2 = 0.65$ with OC and 0.72 with EC) than with ionic compounds ($r^2 = 0.47$–0.59) (Fig. 2). Average OC/EC ratio of 10.3 was much higher than the values reported in previous studies in South Korea (Choi *et al.*, 2021; Park *et al.*, 2021; Yu and Park, 2021), indicating that the portion of secondary OC was significant in this season. Since aged organic matter and secondarily formed organic matter contain more oxygen, which is not analyzed by thermal-optical analysis (Martinez *et al.*, 2012; Turpin and Lim, 2001), organic matter estimated from OC concentration is likely to significantly contribute to $PM_{2.5}$ mass in this city.

In this study, a high concentration episode (HCE) was defined when the measured $PM_{2.5}$ concentrations exceeded 30 μg m^{-3}. Four HCEs occurred during the study period, and a summary of measured data for the HCEs is presented in Table S2. The HCE1, HCE3, and HCE4 showed higher wind speed than the average WS of non-HCEs (Fig. 3), possibly indicating that atmospheric stagnation was not an important factor causing these HCEs. Asian dust event appeared on HCE1, and $PM_{2.5}$/PM_{10} ratio was only 33%, indicating that crustal elements were dominant in the coarse mode. For HCE1, Ca^{2+} and Mg^{2+} concentrations were dramatically enhanced (9.2 times and 4 times higher than the average for Ca^{2+} and Mg^{2+}, respectively), but SO_4^{2-} and NH_4^+ showed even lower concentrations than for non-HCEs (Fig. 3). Increased NO_3^- and OC concentrations for HCE1 (Fig. 3) were probably derived from crustal sources (Lee *et al.*, 2014). The Σn-alkane also showed the highest concentration in HCE1 (Fig. 3), suggesting that soil resuspension affected these non-polar organic compounds, as found in previous research efforts (Alves *et al.*, 2016). The ΣPAHs in HCE1 was higher than in non-HCE, and CHR and BkF, known as the major PAHs in temperate soil (Wilcke, 2000), increased the most (2.0 and 2.3 times higher for HCE1 than the average during the entire sampling period).
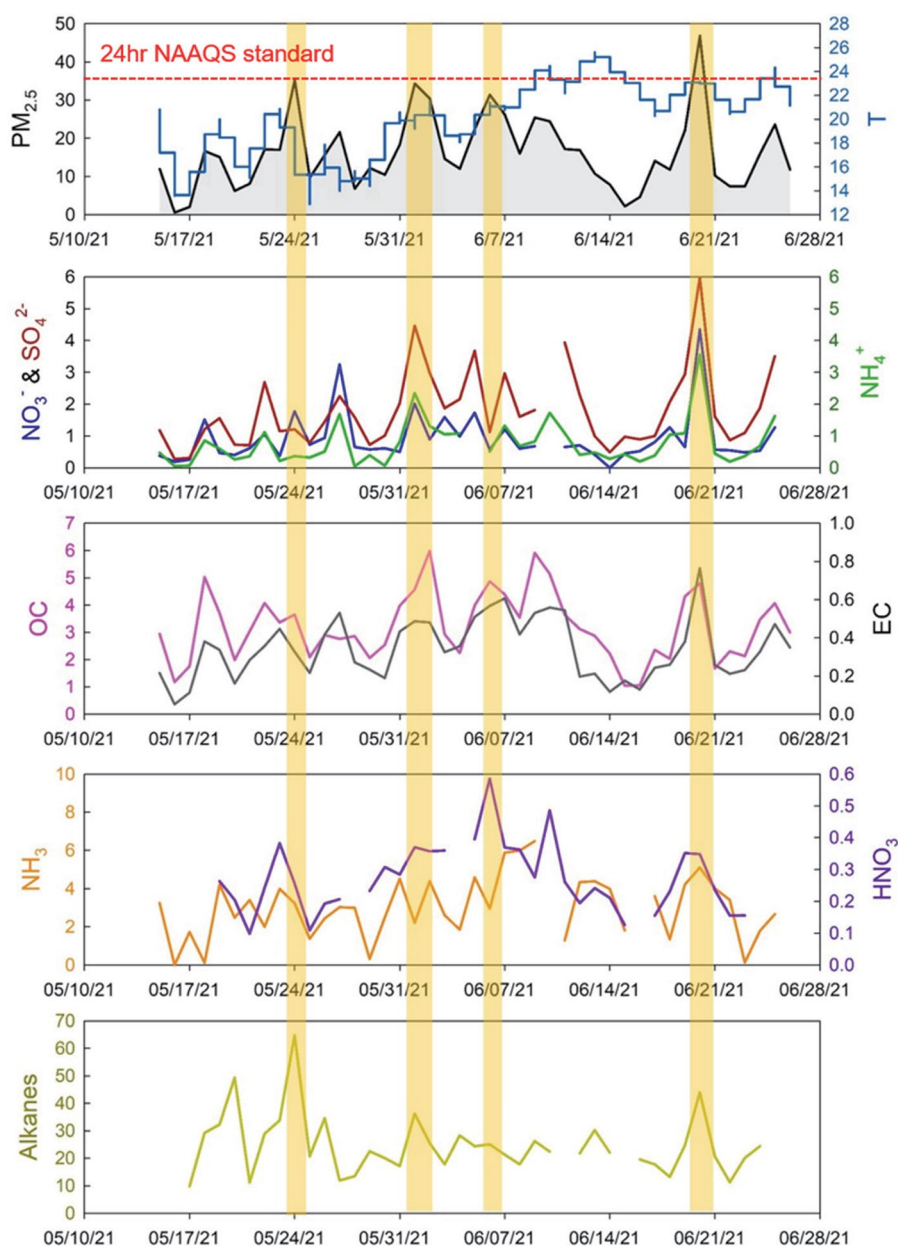
Fig. 2. Daily variation of PM$_{2.5}$ and its major chemical constituents. The four high concentration events (HCEs) of PM$_{2.5}$ are indicated as thick yellow lines. The red dashed line in the top panel indicates the 24-h national ambient air quality standard (NAAQS) of Korea.

On the other hand, low wind speed (WS) and high relative humidity (RH) were observed for HCE2 (Fig. 3), providing suitable aqueous heterogeneous reactions. Both HCE2 and HCE4 showed significantly increased ionic constituents, but NO$_3^-$ of HCE2 did not increase as much as that of HCE4, while SO$_4^{2-}$ and NH$_4^+$ were dramatically enhanced for both HCE2 and HCE4. The reaction rate of NO$_2$ with OH is an order of magnitude greater than that of SO$_2$ with OH (Ma *et al.*, 2021; Seinfeld

and Pandis, 2016), while heterogeneous chemistry was frequently found to be more important than gas-phase oxidation for the SO$_4^{2-}$ formation mechanism (Zheng *et al.*, 2015). High RH and low WS observed for the HCE2 possibly suggested that aqueous reactions played more important roles in SO$_4^{2-}$ formation than in NO$_3^-$ formation at this site. In the meantime, HCE4 showed largest increases on NO$_3^-$, SO$_4^{2-}$, and NH$_4^+$, as well as on gaseous O$_3$ concentration; therefore, gas-phase oxidation
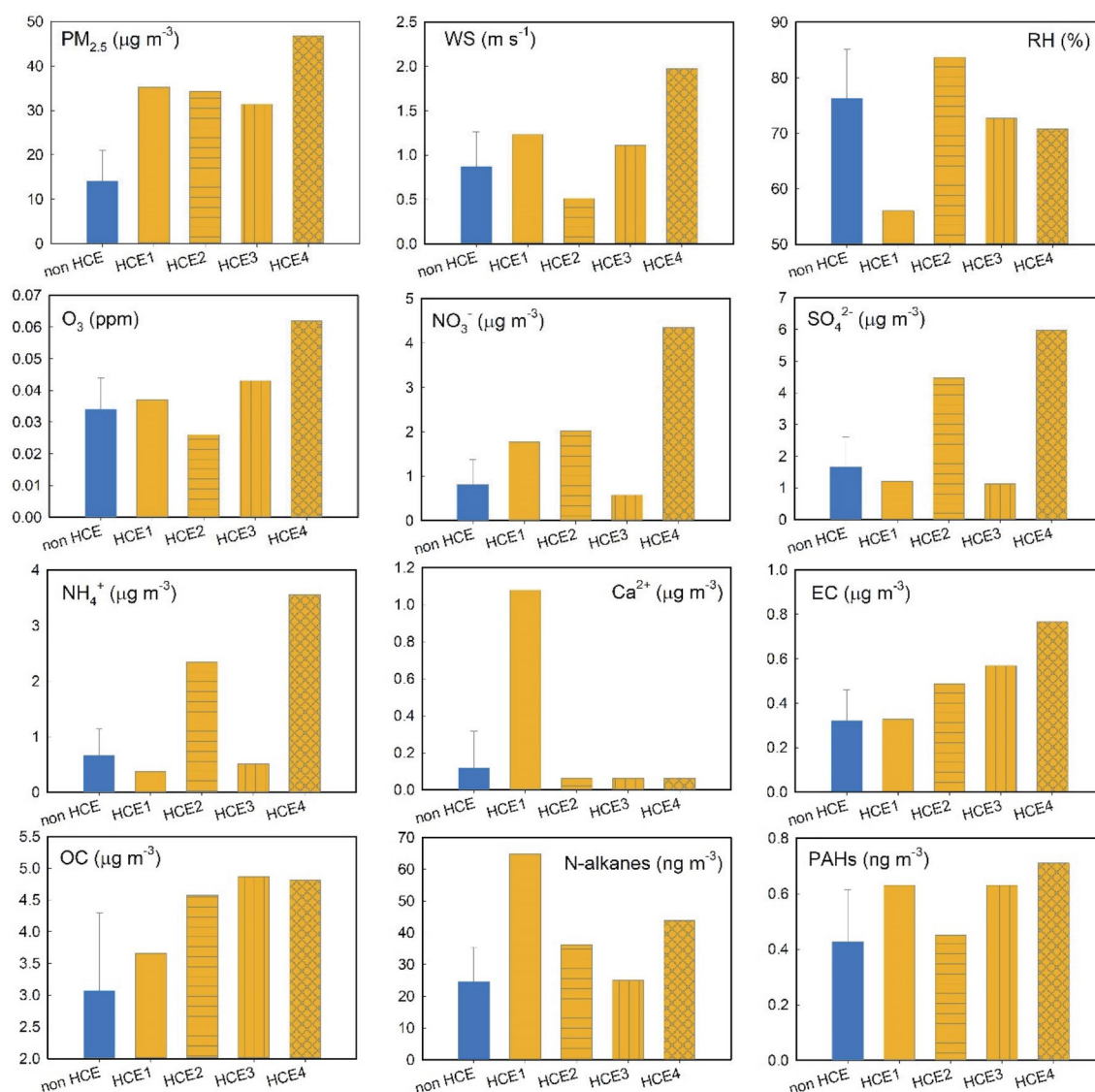
Fig. 3. $PM_{2.5}$ component characteristics with wind speed and relative humidity for each HCE event. O_3 concentrations were obtained from the nearest national ambient air monitoring station.

mechanisms were significant, as O_3 is predominantly produced via a series of gas-phase reactions (Sun *et al.*, 2011), which is also supported by the significant negative correlation between RH and O_3 observed in this study (Pearson r = 0.47, p-value < 0.001). The OC also significantly increased for both HCE2 and HCE4, but the relative increment rate in OC to EC concentrations was large for HCE2, compared with HCE4 (Fig. 3), suggesting that secondary OC formation was likely to be more important for HCE2 than for HCE4. The $PM_{2.5}/PM_{10}$ ratios for both HCE2 (88%) and HCE4 (94%) were also very high, supporting the importance of secondary aerosol forma-

tion. On the other hand, in HCE3, the concentrations of ionic constituents were rather reduced, while OC and EC increased about 1.5 and 1.9 times the average concentrations of non-HCEs (Fig. 3), suggesting that the primary sources emitting carbonaceous compounds played an important role in enhancing $PM_{2.5}$ concentration. Variation of ΣPAHs from HCE2 to HCE4 was similar to EC variation (Fig. 3).

To identify the possible source areas, backward trajectories for the top 10% of $PM_{2.5}$ were compared with those for the bottom 10% of $PM_{2.5}$. Back-trajectories associated with the top 10% of $PM_{2.5}$ were clearly distinct from

those of the bottom 10% of PM$_{2.5}$, showing that high PM$_{2.5}$ samples originated from northeastern China, and passed through the western metropolitan area and industrial areas of Korea (Fig. S1 of the SI).

3.2 Characteristics of Ionic Compounds

The highest average concentration among PM$_{2.5}$ ionic constituents was shown by SO$_4^{2-}$ (1.8 µg m^{-3}), followed by NO$_3^-$ (0.9 µg m^{-3}) and NH$_4^+$ (0.8 µg m^{-3}). The neutralization ratio (NR) was calculated to describe the aerosol acidity:

$$NR = \frac{[NH_4^+]}{[SO_4^{2-}] + [NO_3^-]} \tag{1}$$

where, concentrations are in equivalents. The [NH$_4^+$] and [SO$_4^{2-}$] + [NO$_3^-$] were highly correlated with each other, indicating that most ionic compounds existed as NH$_4$NO$_2$ and (NH$_4$)$_2$SO$_4$ (Fig. 4a). Average NR was (0.72 ± 0.26), indicating slightly acidic aerosols (Fig 4a). To investigate the degree of neutralization of secondary inorganic aerosol (SIA), NR was plotted according to the NH$_4^+$ concentration (Fig. 4b). When NH$_4^+$ exceeded about 50 nmole m^{-3}, the NR appeared constant around 1, and SIA was completely neutralized. In other cases, NR almost linearly increased as NH$_4^+$ increased, possibly indicating that NH$_3$ was the limiting factor for SIA formation in this study. The HCE2 and HCE4, where SIA concentration was significantly enhanced (Fig. 3), showed the highest NR values (1.04 and 1.01, respective-

ly) over the entire period, suggesting that NH$_3$ was likely to cause high PM$_{2.5}$ concentrations.

The PM$_{2.5}$ component that increased the most during HCEs appeared to be NO$_3^-$ on average. To identify the influence of NO$_2$ and SO$_2$ on NO$_3^-$ and SO$_4^{2-}$ formations, respectively, the sulfur oxidation ratio (SOR) and the nitrogen oxidation ratio (NOR) were calculated:

$$SOR = \frac{[SO_4^{2-}]}{[SO_4^{2-}] + [SO_2]} \tag{2}$$

$$NOR = \frac{[NO_3^-]}{[NO_3^-] + [NO_2]} \tag{3}$$

where, [SO$_4^{2-}$], [SO$_2$], [NO$_3^-$], and [NO$_2$] refer to the molar concentrations. In this study, SOR considers only the aerosol fraction since H$_2$SO$_4$ was not measured, but HNO$_3$ was considered for the total [NO$_3^-$] (T-NO$_3^-$) in NOR. The average SOR (of 0.20 ± 0.10) was higher than the average NOR (of 0.08 ± 0.04), but the NOR and the SOR during HCEs increased about 2.3 and 1.5 times, compared to those during non-HCEs, respectively. To determine whether the gaseous precursors of NO$_2$ and SO$_2$ were oxidized to form SIA, the correlation between NO$_2$ and T-NO$_3^-$ and between SO$_2$ and SO$_4^{2-}$ were investigated. Both regressions were significant (p-values < 0.001), but the r^2 was much higher between NO$_2$ and T-NO$_3^-$ than between SO$_2$ and SO$_4^{2-}$ (please note that one outlier, indicated as red point in Fig. 5, was excluded for the regression between NO$_2$ and T-NO$_3^-$). These
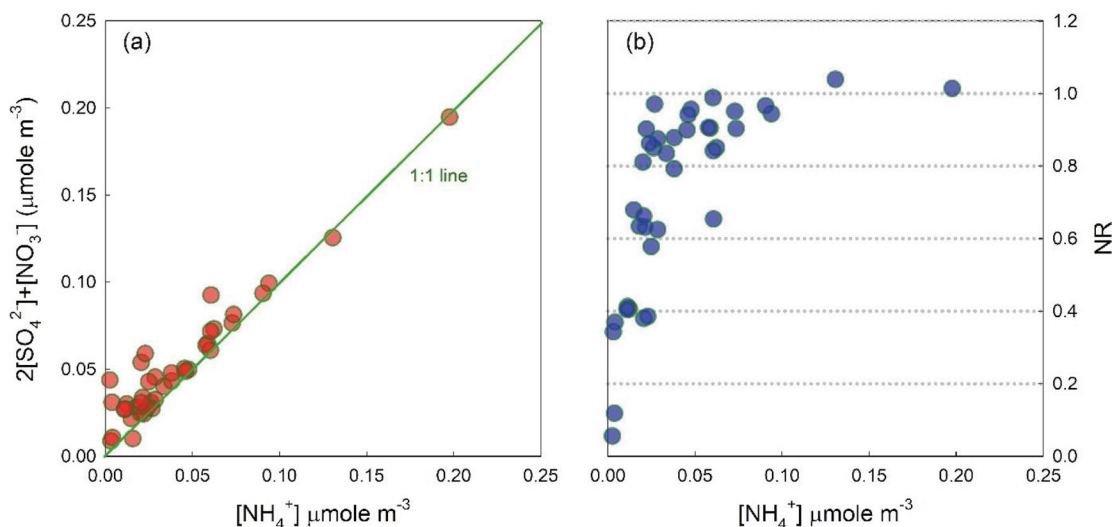

Fig. 4. Correlation between the molar concentrations of [NH$_4^+$] and 2[SO$_4^{2-}$] + [NO$_3^-$] (left), and the change of NR ratio according to NH$_4^+$ concentration.
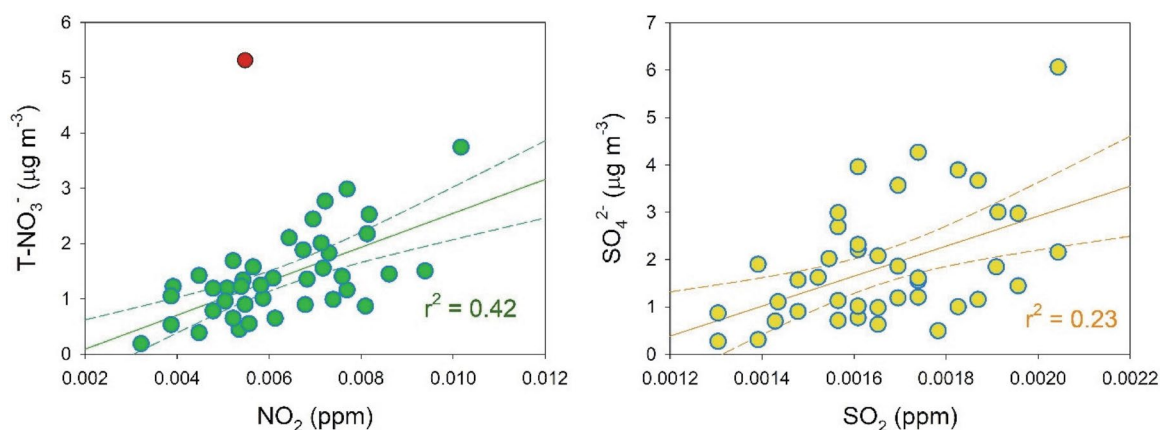
Fig. 5. Influence of gaseous NO_2 on total NO_3^- (left) and gaseous SO_2 on SO_4^{2-} concentration (right).

results possibly indicate that *in situ* oxidation of NO_2 and/or gas-aerosol partitioning for HNO_3 and NO_3^- occurred, even in the relatively warm season.

3. 3 Nonpolar Organic Compounds

N-alkanes are common organic compounds in $PM_{2.5}$, emitted from both anthropogenic and natural sources (Rogge *et al.*, 1993; Simoneit, 1986). In this study, average Σn-alkane concentration was (24.5 ± 11.0) ng m^{-3}, and there was relatively strong correlation between Σn-alkane and $PM_{2.5}$ concentrations (Pearson r = 0.47). The average concentrations of Σn-alkane were 14.0 ± 10.3 ng m^{-3} and 53.7 ± 35.0 ng m^{-3} at the background site (Anmyeon Island) (Kim *et al.*, 2018) and in Seoul (Lee *et al.*, 2015), respectively, indicating that the Σn-alkane concentrations reported in this study were relatively higher than in Anmyeon Island and lower than in Seoul. The C29 (n-nonacosane) and C31 (n-hentriacontane) were the most abundant species with the largest coefficient of variation (standard deviation divided arithmetic mean) (Fig. 6). Previous studies suggested that high carbon numbers generally appear from biogenic sources, including plant wax and bacteria, while low carbon numbers indicate a large contribution from fossil fuel combustion (Sun *et al.*, 2021; Chen *et al.*, 2014; Feng *et al.*, 2006). Other research shows that C_{max} ranges (C18 to C22) for petrol vehicles, and is C21 for diesel vehicles (Zhang *et al.*, 2021). In this study, the relative concentration of C20–C23 was lower than the higher molecular weight alkanes (Fig. 6), indicating that fossil fuel combustion was not important. The carbon preference index (CPI, Eq. (8)) has often been used to identify the alkanes from

natural emissions from the alkanes from anthropogenic emissions, because odd alkanes, rather than even alkanes, were preferred for biogenic sources.

$$CPI = \frac{\Sigma \text{ total odd number of carbons}}{\Sigma \text{ total even number of carbons}} \quad (4)$$

When CPI is close to 1, n-alkanes are mainly from anthropogenic sources, such as fossil fuel combustion and biomass burning, because the emission distribution of even and odd alkanes from these sources is not selective (Gao *et al.*, 2022; Choi *et al.*, 2012). When $1 < CPI < 3$, n-alkanes are influenced by both biogenic and anthropogenic sources, and a higher CPI indicates a higher effect of biogenic sources (Feng *et al.*, 2021). In this study, odd alkanes generally showed higher abundance than even alkanes (Fig. 6), suggesting the importance of biogenic sources over fossil fuel combustion. Average CPI value was (1.73 ± 0.92) with relatively large variation, ranging $(0.57$ to $3.99)$, and the two maximum CPIs were observed on May 24 and May 26 when the $PM_{2.5}/PM_{10}$ ratio was $(0.33$ and $0.39)$, respectively, indicating that natural sources were more significant than combustion source. Asian dust event occurred on May 24 when the highest Σn-alkane concentration $(64.8$ ng m$^{-3})$ appeared during the sampling period (Fig. 2).

Relatively high Σn-alkane concentrations were shown for HCEs (Fig. 3), but the relative abundance of each alkane varied. For HCE1 and HCE3, the odd alkanes of C27, C29, and C31 were dominant, contributing $(65$ and $48)\%$, respectively (Fig. 6). According to Li *et al.* (2010), alkanes are anticipated to be mainly emitted from biogenic sources if the odd alkanes among C27–C31 are
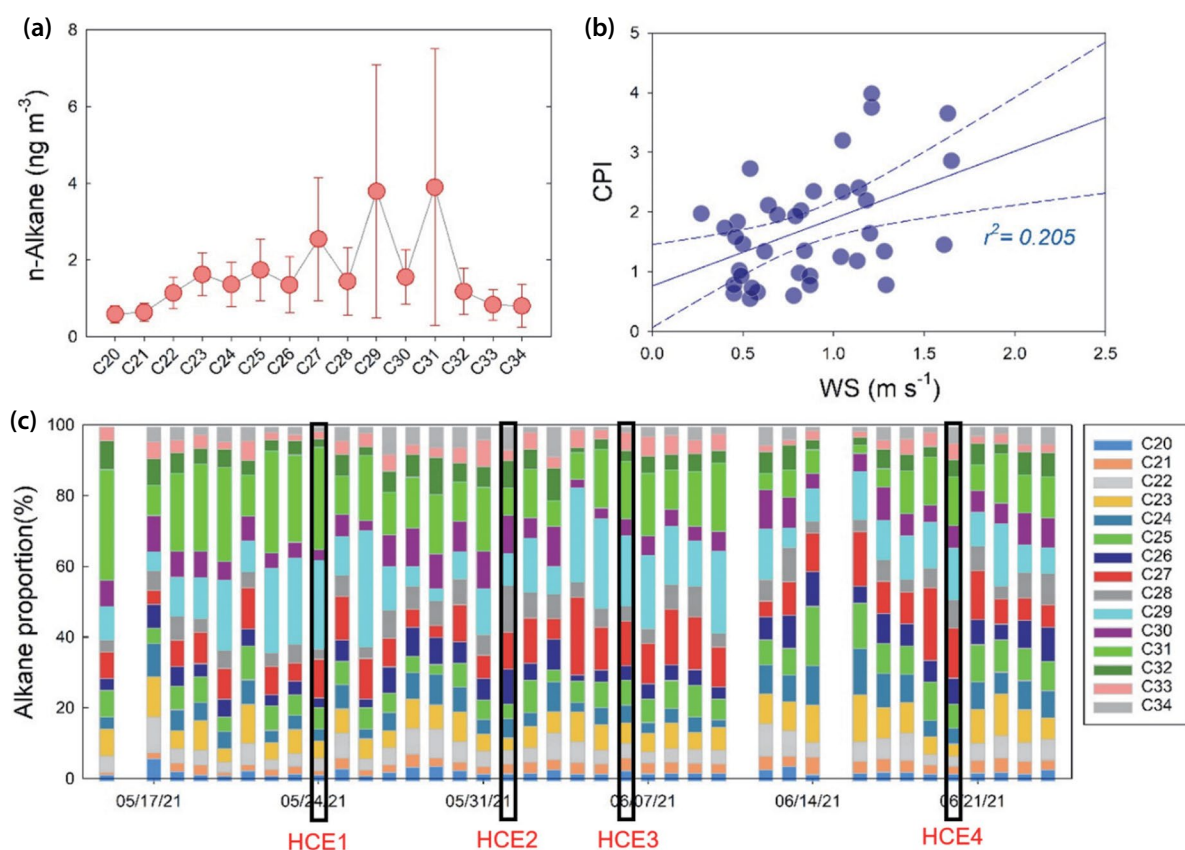
Fig. 6. (a) Abundance of n-alkanes, (b) the relationship between wind speed and CPI value, and (c) the daily variation of C$_{max}$ proportion.

higher than even alkanes. In HCE3, the concentrations of ionic constituents were low, while the highest OC concentration was shown among all HCEs (Fig. 3), and high CPI of 2.35 was observed; therefore, the high OC of HCE3 was partly influenced by biogenic sources, such as plant wax and microorganism. On the other hand, for both HCE2 and HCE4 categorized by SIA-derived event (Fig. 3), CPI values were relatively low at (0.68 and 1.47), respectively.

In this study, CPI was statistically correlated with WS (Pearson r = 0.45) (Fig. 6), suggesting that the biogenic alkanes were significantly emitted from epicuticular wax with the effect of strong wind (Thao *et al.*, 2014). Previous study also found that up to 50% of the leaf surface wax was lost after strong winds (Hall and Donaldson, 1963).

Average ΣPAHs concentration was (0.43 ± 0.19) ng m^{-3}, and there was statistically significant (at a significance level of 0.05), but not high, correlation between ΣPAHs and Σn-alkane (Pearson r = 0.38, p-value = 0.019). Among 11 PAHs measured, PYR and BbF showed the

highest average concentrations of 0.08 ng m^{-3}. All PAHs concentrations were significantly lower than those measured at the same sampling site in 2014–2015 (Park *et al.*, 2018). Previous studies showed that PAHs concentrations have dramatically decreased recently in other cities in Korea and in China (Zhang *et al.*, 2021; Kang *et al.*, 2020). In Seoul, the measured ΣPAHs concentration in 2018 were approximately one-fifth that of 2002, and the decreasing trend was more pronounced in summer (decreasing from 6.8 ng m^{-3} in 2002 to 0.8 ng m^{-3} in 2018 during summer) (Kang *et al.*, 2020). The PAHs concentrations typically show clear seasonal variation with high values in winter and low values in summer (Shin *et al.*, 2022; Nguyen *et al.*, 2018; Ma *et al.*, 2010), and low PAHs concentrations in this study were also likely to be reflected by seasonal influences. Concentrations of high molecular weight (HMW)-PAHs exceeded the medium-MW (MMW)-PAHs and low-MW (LMW)-PAHs in this study, indicating that vehicular emissions were more important than solid fuel combustion (Ali-Taleshi *et al.*, 2021), or that LMW-PAHs showed much lower gas-par-
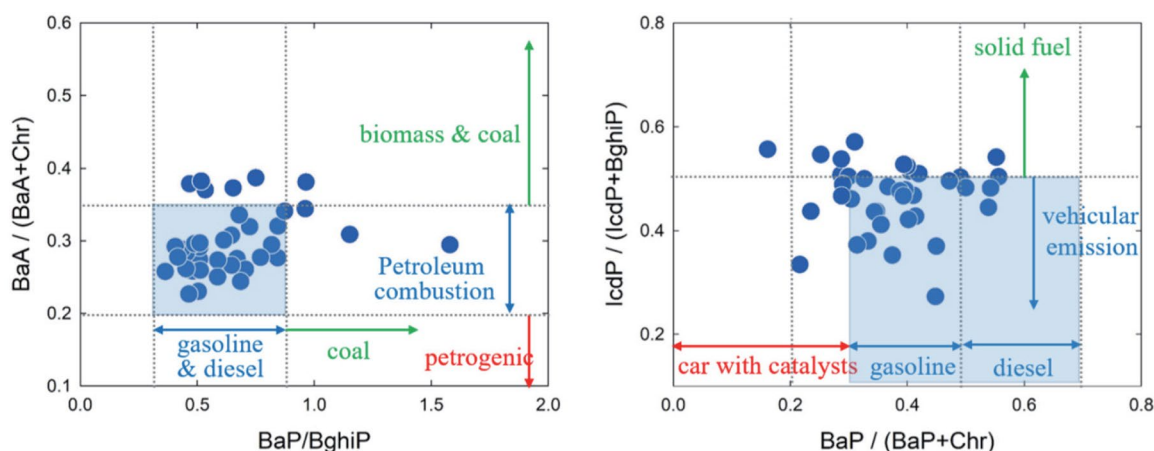
Fig. 7. Diagnostic ratios to identify the major sources of PAHs. Results in this study generally suggest that the vehicular emissions were important.

ticle partitioning coefficient, K_p than HMW-PAHs, especially in the warm season (Chen *et al.*, 2016; Venkataraman *et al.*, 1999).

Since PAH composition profiles are characteristics of each specific emission source, the diagnostic ratios (DRs) can be used to identify the source types. In this study, four DRs were used, of BaA/(BaA+Chr), BaP/BghiP, BaP (BaP+Chr), and IcdP/(IcdP+BghiP). BaA/(BaA+Chr) less than 0.2 indicates a petrogenic source, while it ranges (0.2 to 0.35) for petroleum combustion (Kang *et al.*, 2020; Finardi *et al.*, 2017; Simcik *et al.*, 1999). In this study, the BaA/(BaA+Chr) was in the range (0.2 to 0.35) for most samples (Fig. 7), indicating the influence of vehicular emission. The BaP/BghiP ratio can further identify PAHs from gasoline (0.3–0.45) and diesel (0.45–0.8) (Zhang *et al.*, 2021), indicating the major influence of diesel vehicle in this study (Fig. 7). The IcdP/(IdcP+BghiP) less than 0.5 and BaP/(BaP+Chr) ranging (0.3 to 0.7) indicate vehicular emission (Liu *et al.*, 2017). A similar domestic study conducted using the PAHs diagnostic ratio showed that PAHs were greatly affected by vehicular emission in Seoul during summer (Kang *et al.*, 2020). Previous study conducted at the same sampling site as this study showed that solid-fuel combustion, including biomass and coal burning, was predominant source of PAHs in winter (Park *et al.*, 2018).

There are some discrepancies for DR values in characterizing the different sources in the scientific literature; however, it was generally speculated that PAHs were majorly influenced by vehicular emission, although some influence of solid fuel combustion, such as coal and bio-

mass burning, was observed in this study (Fig. 7). The DRs are better to be used with consideration of different volatilities of compounds, to reduce the impact of ambient temperature (Shen *et al.*, 2019); however, the ratio of BaP/(BaP+Chr), which does not meet this rule, was considered, because all samples were collected in the relatively warm season (May and June).

4. CONCLUSIONS

Haze caused by high $PM_{2.5}$ concentration is a serious air pollution event in East Asia. The formation pathways and major sources of $PM_{2.5}$ greatly vary spatially and temporally, with different proportions of $PM_{2.5}$ components. Therefore, even exposure to the same $PM_{2.5}$ mass concentration may have different health effects from region to region. In this study, the chemical constituents of $PM_{2.5}$ were measured in a small residential city of South Korea during May and June, 2021, to identify the cause of high $PM_{2.5}$ concentration. Average $PM_{2.5}$ concentration was $16.4 \pm 9.7 \, \mu g \, m^{-3}$, and OC was the largest contributor on average, followed by SO_4^{2-} and NO_3^-. There were four $PM_{2.5}$ episodes exceeding $30 \, \mu g \, m^{-3}$, which were characterized as one Asian dust event, two SIA events, and one OC event. The neutralization ratio (NR) calculated by molar concentrations of SO_4^{2-}, NO_3^-, and NH_4^+ linearly increased as NH_4^+ increased, until NR appeared constant around 1, suggesting that NH_3 was the limiting factor for SIA formation.

Since OC is the primary component of $PM_{2.5}$ in this

area, identification of its possible sources is an important task. There was relatively strong correlation between n-alkanes and PM$_{2.5}$, and odd alkanes including C27, C29, and C31, which are generally emitted from biogenic sources, were the most abundant species, indicating that the natural sources are possibly important to PM$_{2.5}$ concentration in this study. The PAHs were also measured, and their concentrations were significantly lower than those measured at the same sampling site in 2014 and 2015, which shows the same decreasing trends as in other cities in Korea, and in China. Based on the DR result of PAHs, vehicular emissions, rather than solid fuel emissions, were significant.

AUTHOR CONTRIBUTIONS

The work presented in this article was carried out through collaboration between all authors. S.-W.P. analyzed the data and wrote the paper. J.-H.H. performed the experiments. Y.-J.H. acquired the funding, defined the research theme, interpreted the results, and wrote the paper. T.-H.L. partly acquired the funding.

ACKNOWLEDGEMENT

REFERENCES

Ali-Taleshi, M.S., Squizzato, S., Riyahi Bakhtiari, A., Moeinaddini, M., Masiol, M. (2021) Using a hybrid approach to apportion potential source locations contributing to excess cancer risk of PM$_{2.5}$-bound PAHs during heating and non-heating periods in a megacity in the Middle East. Environmental Research, 201, 111617. https://doi.org/10.1016/j.envres.2021.111617

Alves, C.A., Oliveira, C., Martins, N., Mirante, F., Caseiro, A., Pio, C., Matos, M., Silva, H.F., Oliveira, C., Camões, F. (2016) Road tunnel, roadside, and urban background measurements of aliphatic compounds in size-segregated particulate matter. Atmospheric Research, 168, 139–148. https://doi.org/10.1016/j.atmosres.2015.09.007

Atkinson, R.W., Kang, S., Anderson, H.R., Mills, I.C., Walton, H.A. (2014) Epidemiological time series studies of PM$_{2.5}$ and daily mortality and hospital admissions: a systematic review and meta-analysis. Thorax, 69(7), 660–665. https://doi.org/10.1136/thoraxjnl-2013-204492

Byun, J.-Y., Kim, H., Han, Y.-J., Lee, S.-D., Park, S.-W. (2020) High PM$_{2.5}$ Concentrations in a Small Residential City with Low Anthropogenic Emissions in South Korea. Atmosphere, 11(11), 1159. https://doi.org/10.3390/atmos11111159

Chen, Y., Cao, J., Zhao, J., Xu, H., Arimoto, R., Wang, G., Han, Y., Shen, Z., Li, G. (2014) N-alkanes and polycyclic aromatic hydrocarbons in total suspended particulates from the southeastern Tibetan Plateau: concentrations, seasonal variations, and sources. Science of The Total Environment, 470–471, 9–18. https://doi.org/10.1016/j.scitotenv.2013.09.033

Chen, Y.C., Chiang, H.C., Hsu, C.Y., Yang, T.T., Lin, T.Y., Chen, M.J., Chen, N.T., Wu, Y.S. (2016) Ambient PM$_{2.5}$-bound polycyclic aromatic hydrocarbons (PAHs) in Changhua County, central Taiwan: Seasonal variation, source apportionment and cancer risk assessment. Environmental Pollution, 218, 372–382. https://doi.org/10.1016/j.envpol.2016.07.016

Choi, J.-K., Heo, J.-B., Ban, S.-J., Yi, S.-M., Zoh, K.-D. (2012) Chemical characteristics of PM$_{2.5}$ aerosol in Incheon, Korea. Atmospheric Environment, 60, 583–592. https://doi.org/10.1016/j.atmosenv.2012.06.078

Choi, S.-Y., Lee, H.-J., Park, S.-W., Han, Y.-J. (2022) Enhanced PM$_{2.5}$ episodes in a small residential city of South Korea: Effects of biomass burning and secondary formations. Atmospheric Pollution Research, 13(10), 101562. https://doi.org/10.1016/j.apr.2022.101562

Choi, S.-Y., Park, S.-W., Byun, J.-Y., Han, Y.-J. (2021) Characteristics of locally occurring high PM$_{2.5}$ concentration episodes in a small city in south korea. Atmosphere, 12(1), 86. https://doi.org/10.3390/atmos12010086

Dominici, F., Peng, R.D., Bell, M.L., Pham, L., McDermott, A., Zeger, S.L., Samet, J.M. (2006) Fine particulate air pollution and hospital admission for cardiovascular and respiratory diseases. Jama, 295(10), 1127–1134. https://doi.org/10.1001/jama.295.10.1127

Feng, J., Hu, M., Chan, C.K., Lau, P.S., Fang, M., He, L., Tang, X. (2006) A comparative study of the organic matter in PM$_{2.5}$ from three Chinese megacities in three different climatic zones. Atmospheric Environment, 40(21), 3983–3994. https://doi.org/10.1016/j.atmosenv.2006.02.017

Feng, T., Wang, F., Yang, F., Li, Z., Lu, P., Guo, Z. (2021) Carbonaceous aerosols in urban Chongqing, China: Seasonal variation, source apportionment, and long-range transport. Chemosphere, 285, 131462. https://doi.org/10.1016/j.chemosphere.2021.131462

Finardi, S., Radice, P., Cecinato, A., Gariazzo, C., Gherardi, M., Romagnoli, P. (2017) Seasonal variation of PAHs concentration and source attribution through diagnostic ratios analysis. Urban Climate, 22, 19–34. https://doi.org/10.1016/j.uclim.2015.12.001

Gao, X., Yang, L., Cheng, S., Gao, R., Zhou, Y., Xue, L., Shou, Y., Wang, J., Wang, X., Nie, W., Xu, P., Wang, W. (2011) Semi-

continuous measurement of water-soluble ions in PM$_{2.5}$ in Jinan, China: Temporal variations and source apportionments. Atmospheric Environment, 45(33), 6048–6056. https://doi.org/10.1016/j.atmosenv.2011.07.041

Gao, Y., Ling, Z., Zhang, Z., Lee, S. (2022) Characteristics of Fine Particulate Matter (PM$_{2.5}$)-Bound n-Alkanes and Polycyclic Aromatic Hydrocarbons (PAHs) in a Hong Kong Suburban Area. Atmosphere, 13(6), 980. https://doi.org/10.3390/atmos13060980

Hall, D., Donaldson, L. (1963) The ultrastructure of wax deposits on plant leaf surfaces: I. Growth of wax on leaves of Trifolium repens. Journal of Ultrastructure Research, 9(3–4), 259–267. https://doi.org/10.1016/S0022-5320(63)80006-4

Hoek, G., Krishnan, R.M., Beelen, R., Peters, A., Ostro, B., Brunekreef, B., Kaufman, J.D. (2013) Long-term air pollution exposure and cardio-respiratory mortality: a review. Environmental Health, 12(1), 1–16. https://doi.org/10.1186/1476-069X-12-43

Kang, M., Kim, K., Choi, N., Kim, Y.P., Lee, J.Y. (2020) Recent Occurrence of PAHs and n-Alkanes in PM$_{2.5}$ in Seoul, Korea and Characteristics of their Sources and Toxicity. International Journal of Environmental Research and Public Health, 17(4), 1397. https://doi.org/10.3390/ijerph17041397

Kim, K.A., Lee, J.S., Kim, E.S., Jung, C.H., Kim, Y.P., Lee, J.Y. (2018) Monthly Variation of n-alkanes concentration in PM$_{2.5}$ of the Anmyeon Island. Journal of Korean Society for Atmospheric Environment, 34(1), 166–176. https://doi.org/10.5572/kosae.2018.34.1.166

Kotianová, P., Puxbaum, H., Bauer, H., Caseiro, A., Marr, I.L., Čík, G. (2008) Temporal patterns of n-alkanes at traffic exposed and suburban sites in Vienna. Atmospheric Environment, 42(13), 2993–3005.

Lee, S., Kim, J., Choi, M., Hong, J., Lim, H., Eck, T.F., Holben, B.N., Ahn, J.-Y., Kim, J., Koo, J.-H. (2019) Analysis of long-range transboundary transport (LRTT) effect on Korean aerosol pollution during the KORUS-AQ campaign. Atmospheric Environment, 204, 53–67. https://doi.org/10.1016/j.atmosenv.2019.02.020

Lee, S.P., Lim, H.B., Lee, J.Y., Kim, Y.P. (2015) Seasonal Variation of Concentrations and Sources for n-alkanes in PM$_{10}$ Measured in Seoul. Journal of Korea Society for Environmental Analysis, 18(2), 93–100.

Lee, Y.-J., Jung, S.-A., Jo, M.-R., Kim, S.-J., Park, M.-K., Ahn, J.-Y., Lyu, Y.-S., Choi, W.-J., Hong, Y.-D., Han, J.-S. (2014) Characteristics of PM chemical component during haze episode and Asian dust at Gwang-ju. Journal of Korean Society for Atmospheric Environment, 30(5), 434–448. https://doi.org/10.5572/KOSAE.2014.30.5.434

Li, K., Jacob, D.J., Shen, L., Lu, X., De Smedt, I., Liao, H. (2020) Increases in surface ozone pollution in China from 2013 to 2019: anthropogenic and meteorological influences. Atmospheric Chemistry and Physics, 20(19), 11423–11433. https://doi.org/10.5194/acp-20-11423-2020

Liu, J., Wang, Y., Li, P.-H., Shou, Y.-P., Li, T., Yang, M.-M., Wang, L., Yue, J.-J., Yi, X.-L., Guo, L.-Q. (2017) Polycyclic Aromatic Hydrocarbons (PAHs) at High Mountain Site in North China: Concentration, Source and Health Risk Assessment.

Aerosol and Air Quality Research, 17(11), 2867–2877. https://doi.org/10.4209/aaqr.2017.08.0288

Ma, P., Quan, J., Jia, X., Liao, Z., Wang, Q., Cheng, Z., Dou, Y., Su, J., Pan, Y. (2021) Effects of ozone and relative humidity in secondary inorganic aerosol formation during haze events in Beijing, China. Atmospheric Research, 264, 105855. https://doi.org/10.1016/j.atmosres.2021.105855

Ma, W.L., Li, Y.F., Qi, H., Sun, D.Z., Liu, L.Y., Wang, D.G. (2010) Seasonal variations of sources of polycyclic aromatic hydrocarbons (PAHs) to a northeastern urban city, China. Chemosphere, 79(4), 441–447. https://doi.org/10.1016/j.chemosphere.2010.01.048

Martinez, M.A., Caballero, P., Carrillo, O., Mendoza, A., Mejia, G.M. (2012) Chemical characterization and factor analysis of PM$_{2.5}$ in two sites of Monterrey, Mexico. Journal of Air & Waste Management Association, 62(7), 817–827. https://doi.org/10.1080/10962247.2012.681421

National Institute of Environmental Research (NIER) (2011) QA/QC Handbook for the Environmental Pollutants Analysis and Sampling Techniques. https://ecolibrary.me.go.kr/nier/#/search/detail/5508913

National Institute of Environmental Research (NIER) (2022a) Annual Report of Air Quality in Korea, 2021. https://www.airkorea.or.kr/web/detailViewDown?pMENU_NO=125

National Institute of Environmental Research (NIER) (2022b) 2019 national air pollutant emissions. https://www.air.go.kr/article/view.do?boardId=7&articleId=145&boardId=7&menuId=48&currentPageNo=1

Nguyen, T.N.T., Jung, K.S., Son, J.M., Kwon, H.O., Choi, S.D. (2018) Seasonal variation, phase distribution, and source identification of atmospheric polycyclic aromatic hydrocarbons at a semi-rural site in Ulsan, South Korea. Environmental Pollution, 236, 529–539. https://doi.org/10.1016/j.envpol.2018.01.080

Park, J.-M., Han, Y.-J., Cho, S.-H., Kim, H.-W. (2018) Characteristics of Carbonaceous PM$_{2.5}$ in a Small Residential City in Korea. Atmosphere, 9(12), 490. https://doi.org/10.3390/atmos9120490

Park, S.-W., Choi, S.-Y., Byun, J.-Y., Kim, H., Kim, W.-J., Kim, P.-R., Han, Y.-J. (2021) Different Characteristics of PM$_{2.5}$ Measured in Downtown and Suburban Areas of a Medium-Sized City in South Korea. Atmosphere, 12(7), 832. https://doi.org/10.3390/atmos12070832

Pun, V.C., Kazemiparkouhi, F., Manjourides, J., Suh, H.H. (2017) Long-Term PM$_{2.5}$ Exposure and Respiratory, Cancer, and Cardiovascular Mortality in Older US Adults. American Journal of Epidemiology, 186(8), 961–969. https://doi.org/10.1093/aje/kwx166

Rogge, W.F., Hildemann, L.M., Mazurek, M.A., Cass, G.R., Simoneit, B.R. (1993) Sources of fine organic aerosol. 4. Particulate abrasion products from leaf surfaces of urban plants. Environmental Science & Technology, 27(13), 2700–2711. https://doi.org/10.1021/es00049a008

Seinfeld, J.H., Pandis, S.N. (2016) Atmospheric Chemistry and Physics: From Air Pollution to Climate Change. Wiley, New York, pp. 1–762.

Shen, R., Liu, Z., Chen, X., Wang, Y., Wang, L., Liu, Y., Li, X. (2019) Atmospheric levels, variations, sources and health

risk of PM$_{2.5}$-bound polycyclic aromatic hydrocarbons during winter over the North China Plain. Science of The Total Environment, 655, 581–590. https://doi.org/10.1016/j.scitotenv.2018.11.220

Shin, S.M., Lee, J.Y., Shin, H.J., Kim, Y.P. (2022) Seasonal variation and source apportionment of Oxygenated Polycyclic Aromatic Hydrocarbons (OPAHs) and Polycyclic Aromatic Hydrocarbons (PAHs) in PM$_{2.5}$ in Seoul, Korea. Atmospheric Environment, 272, 118937. https://doi.org/10.1016/j.atmosenv.2022.118937

Simcik, M.F., Eisenreich, S.J., Lioy, P.J. (1999) Source apportionment and source/sink relationships of PAHs in the coastal atmosphere of Chicago and Lake Michigan. Atmospheric Environment, 33(30), 5071–5079. https://doi.org/10.1016/S1352-2310(99)00233-2

Simoneit, B.R.T. (1986) Characterization of Organic Constituents in Aerosols in Relation to Their rigin and Transport: A Review. International Journal of Environmental Analytical Chemistry, 23(3), 207–237. https://doi.org/10.1080/03067318608076446

Sun, N., Li, X., Ji, Y., Huang, H., Ye, Z., Zhao, Z. (2021) Sources of PM$_{2.5}$-Associated PAHs and n-alkanes in Changzhou China. Atmosphere, 12(9), 1127. https://doi.org/10.3390/atmos12091127

Sun, W.Y., Ding, S.L., Zeng, S.S., Su, S.J., Jiang, W.J. (2011) Simultaneous absorption of NOx and SO$_2$ from flue gas with pyrolusite slurry combined with gas-phase oxidation of NO using ozone. Journal of Hazard Materials, 192(1), 124–130. https://doi.org/10.1016/j.jhazmat.2011.04.104

Thao, N., Yu, X., Zhang, H. (2014) Deposition of particulate matter of different size fractions on leaf surfaces and in epicuticular waxes of urban forest species in summer and fall in Beijing, China. International Journal of Sciences, 3. https://ssrn.com/abstract=2573647

Tsimpidi, A., Karydis, V., Zavala, M., Lei, W., Molina, L., Ulbrich, I., Jimenez, J., Pandis, S.N. (2010) Evaluation of the volatility basis-set approach for the simulation of organic aerosol formation in the Mexico City metropolitan area. Atmospheric Chemistry and Physics, 10(2), 525–546. http://www.atmos-chem-phys.net/10/525/2010/

Turpin, B.J., Lim, H.-J. (2001) Species Contributions to PM$_{2.5}$ Mass Concentrations: Revisiting Common Assumptions for Estimating Organic Mass. Aerosol Science and Technology, 35(1), 602–610. https://doi.org/10.1080/02786820119445

Venkataraman, C., Thomas, S., Kulkarni, P. (1999) Size distribu-

tions of polycyclic aromatic hydrocarbons-gas/particle partitioning to urban aerosols. Journal of Aerosol Science, 30(6), 759–770. https://doi.org/10.1016/S0021-8502(98)00761-7

Wilcke, W. (2000) Synopsis polycyclic aromatic hydrocarbons (PAHs) in soil - a review. Journal of Plant Nutrition and Soil Science, 163(3), 229–248.

Xing, L., Wu, J., Elser, M., Tong, S., Liu, S., Li, X., Liu, L., Cao, J., Zhou, J., El-Haddad, I., Huang, R., Ge, M., Tie, X., Prévôt, A.S.H., Li, G. (2019) Wintertime secondary organic aerosol formation in Beijing - Tianjin - Hebei (BTH): contributions of HONO sources and heterogeneous reactions. Atmospheric Chemistry and Physics, 19(4), 2343–2359. https://doi.org/10.5194/acp-19-2343-2019

Yan, D., Wu, S., Zhou, S., Tong, G., Li, F., Wang, Y., Li, B. (2019) Characteristics, sources and health risk assessment of airborne particulate PAHs in Chinese cities: A review. Environmental Pollution, 248, 804–814.

Yu, G.H., Park, S. (2021) Chemical characterization and source apportionment of PM$_{2.5}$ at an urban site in Gwangju, Korea. Atmospheric Pollution Research, 12(6), 101092. https://doi.org/10.1016/j.apr.2021.101092

Zeng, Y., Cao, Y., Qiao, X., Seyler, B.C., Tang, Y. (2019) Air pollution reduction in China: Recent success but great challenge for the future. Science of The Total Environment, 663, 329–337. https://doi.org/10.1016/j.scitotenv.2019.01.262

Zhang, K., Yang, L., Li, Q., Li, R., Zhang, D., Xu, W., Feng, J., Wang, Q., Wang, W., Huang, L., Yaluk, E.A., Wang, Y., Yu, J.Z., Li, L. (2021) Hourly measurement of PM$_{2.5}$-bound nonpolar organic compounds in Shanghai: Characteristics, sources and health risk assessment. Science of The Total Environment, 789, 148070. https://doi.org/10.1016/j.scitotenv.2021.148070

Zheng, B., Zhang, Q., Zhang, Y., He, K.B., Wang, K., Zheng, G.J., Duan, F.K., Ma, Y.L., Kimoto, T. (2015) Heterogeneous chemistry: a mechanism missing in current models to explain secondary inorganic aerosol formation during the January 2013 haze episode in North China. Atmospheric Chemistry and Physics, 15(4), 2031–2049. https://doi.org/10.5194/acp-15-2031-2015

Zhou, J., Xing, Z., Deng, J., Du, K. (2016) Characterizing and sourcing ambient PM$_{2.5}$ over key emission regions in China I: Water-soluble ions and carbonaceous fractions. Atmospheric Environment, 135, 20–30. https://doi.org/10.1016/j.atmosenv.2016.03.054

SUPPLEMENTARY MATERIALS

Table S1. Analysis condition of GC/MS.

GC 7890A	
Carrier gas	Helium
Gas flow rate	1.0 mL min^{-1}
Column	DB-5MS (30 m long × 0.25 mm ID × 0.1 μm film thickness, diphenyl-dimethyl polysiloxane phase capillary column)
Injection volume	1 μL
Injection mode	Split-less
Inlet temperature	300°C
Initial oven temperature	60°C
Temperature rate	4°C min^{-1}
Hold time	15 min
MSD 5975C	
Electron energy	70 eV
Quadrupole temp.	150°C
Ion source temp.	230°C

Table S2. Summary of the measured data during the four HCE periods.

	Date	WS	RH	PM$_{10}$	PM$_{2.5}$	OC	EC	NO$_3^-$	SO$_4^{2-}$
HCE1	2021-05-24	1.2	56	118	35.3	3.7	0.3	1.8	1.2
HCE2	2021-06-01	0.5	84	38.1	34.3	4.6	0.5	2.0	4.3
HCE3	2021-06-06	1.1	73	52.3	31.4	4.9	0.6	0.6	1.1
HCE4	2021-06-20	2.0	71	52.0	46.8	4.8	0.8	4.4	6.1
	Date	NH$_4^+$	K$^+$	Mg^{2+}	Ca^{2+}	Σn-Alkanes	ΣPAHs	CPI	
HCE1	2021-05-24	0.4	0.104	0.153	1.078	64.8	1.1	3.8	
HCE2	2021-06-01	2.3	0.118	0.019	0.061	36.2	0.5	0.7	
HCE3	2021-06-06	0.5	0.024	0.004	0.062	25.1	0.6	2.4	
HCE4	2021-06-20	3.6	0.143	0.002	0.064	43.9	0.7	1.5	

Note that the unit is in m s^{-1} for WS. The units are ng m^{-3} for n-alkanes and PAHs and μg m^{-3} for all other pollutants.
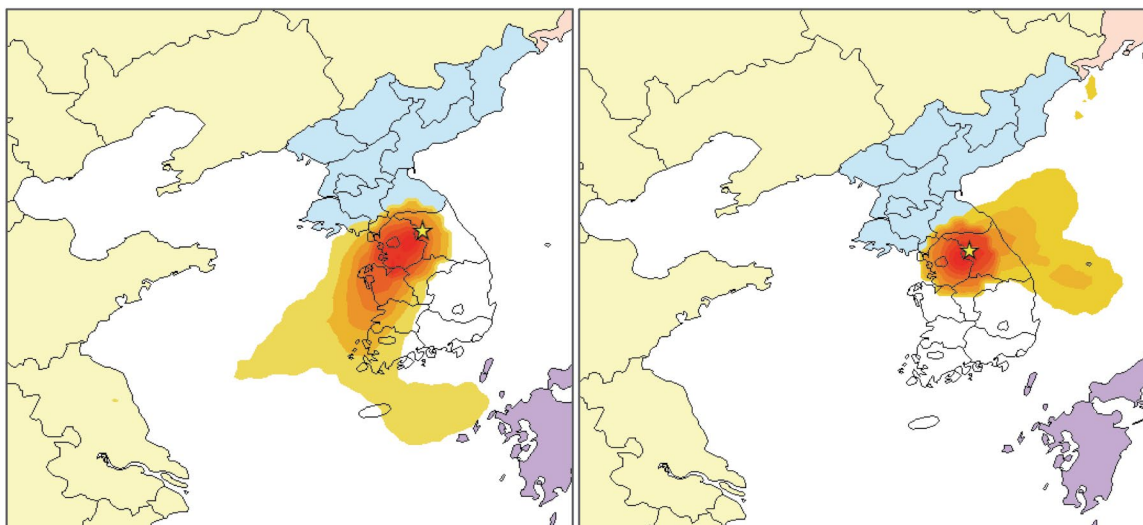
Fig. S1. Residence time of backward trajectories for the top 10% (left) and the bottom 10% of PM$_{2.5}$ mass concentration.